



# Preparing a high-particle-content Ni/diamond composite coating with strong abrasive ability

Wei Huang, Yunwei Zhao, Xiaolei Wang\*

College of Mechanical and Electrical Engineering, Nanjing University of Aeronautics and Astronautics, Nanjing 210016, China  
Jiangsu Key Laboratory of Precision and Micro-Manufacturing Technology, Nanjing 210016, China



## ARTICLE INFO

### Article history:

Received 2 May 2013

Accepted in revised form 4 August 2013

Available online 13 August 2013

### Keywords:

Composite electroplating

Electrophoretic deposition

Nickel

Hardness

Wear

## ABSTRACT

Electrophoretic deposition and electrodeposition techniques are effective methods to increase particle content in composite coatings. In this paper, typical non-conductive diamond and conductive molybdenum disulfide were chosen to fabricate composite coatings using such methods. The results indicate that while Ni/MoS<sub>2</sub> composite coatings cannot be achieved using this method, high-particle-content Ni/diamond coatings can. The surface morphology, particle content and hardness of the Ni/diamond coatings were examined. An anti-wear experiment was performed on the coating under dry sliding conditions in a ball-on-disk tester. The wear resistance of the coatings was evaluated based on the wear rate, and their abrasive ability was assessed by measuring the material removal rate of the corresponding balls.

© 2013 Elsevier B.V. All rights reserved.

## 1. Introduction

Composite electroplating is a method by which micro- or nano-sized particles containing metallic or non-metallic compounds or polymers are co-deposited with a metal or alloy matrix [1]. During the process, these insoluble particles are suspended in a conventional plating electrolyte and captured into the growing metal coatings. Extensive research has been conducted on composite coatings produced using electro-deposition technology because these composite coatings can impart desirable properties, such as resistance to wear [2], corrosion [3–5] and oxidation [6] and self-lubrication [7], to a plated surface.

The concentration of particles incorporated into a coating may fundamentally affect its properties. While deposition coatings created using traditional co-deposition techniques have relatively low particle content [8], the use of low-cost composite electroplating methods continues to expand and addresses the major challenge of achieving high levels of co-deposited particles. Hence, methods to improve the particle concentration in composite coatings have attracted much attention. One common method increases the particle concentration in the bath [9], which undoubtedly increases the cost, especially for precious materials such as diamond particles [10–12]. The Tetsuo Saji group introduced a cost-effective technique for preparing composite coatings with high ceramic particle content using a two-step method [13–15]. The preparation included an electrophoretic deposition of particles followed by an electro/electroless deposition of nickel. Using this method, Ni composite

coatings containing up to 60 vol.% Al<sub>2</sub>O<sub>3</sub> or c-BN ceramic particles could be achieved [13,14]. The question then arises as to whether this method can also be applied to other particles? In addition, how does the performance differ between the coatings fabricated using the two techniques? To date, no results on this subject are available.

In this work, typical non-conductive diamond and conductive molybdenum disulfide were chosen as the composite particles for comparison purposes. We attempted to prepare nickel-based composite coatings via electrophoretic deposition and electrodeposition (using a two-step method). The microstructures and surface morphologies of the final composite coatings were investigated. The indentation and scratch hardness of the coatings were evaluated. The tribological performance of the composite coatings were also compared and analyzed.

## 2. Experimental procedures

### 2.1. Electrophoretic deposition and electrodeposition (two-step method)

Nickel-based composite coatings were fabricated using the electrophoretic deposition and electrodeposition methods. A copper plate with  $\phi 30 \times 3$  mm was used as the cathode and its surface was mechanically polished to Ra 0.1–0.15  $\mu\text{m}$ . The substrate was then activated for 20 s in a mixed acidic bath followed by ultrasonic cleaning with acetone and deionized water for 5 min, respectively. Particles were first electrophoretically deposited on a copper substrate. In the second step, nickel was electrodeposited on this substrate.

The electrophoretic deposition was carried out in a 400-mL beaker in an ethanol bath containing MgCl<sub>2</sub>·6H<sub>2</sub>O (0.2 g/L). The concentration of particles dispersed in the ethanol was 5 g/L. The particles were suspended via ultrasonic agitation for 10 min prior to the deposition.

\* Corresponding author at: College of Mechanical and Electrical Engineering, Nanjing University of Aeronautics and Astronautics, Nanjing 210016, China. Tel./fax: +86 25 84893630.

E-mail address: [wxl@nuaa.edu.cn](mailto:wxl@nuaa.edu.cn) (X. Wang).

The copper plate was aligned vertically at a distance of 1 cm parallel to the 316 stainless steel plate anode. The electrophoretic deposition was performed under a 60-V/cm electric field for 2 min without agitation.

Due to the weak adhesion force between the substrate and the electrophoresis particle film, the substrate covered with the film required careful movement prior to its immersion in a bath for 60 min of nickel electroplating as shown in Table 1, without any particles. After depositing the nickel, the final material was ultrasonically cleaned in acetone and washed with running water.

To determine the differences in the performance, conventional nickel-based composite coatings were fabricated using an organic-free Watts' nickel electrolyte with fine suspended particles and a concentration controlled at 5 g/L. Prior to the co-deposition, the particles were ultrasonically dispersed in the bath for 15 min. In addition, a pure nickel coating was obtained. Specific experimental conditions for the electro-depositions can also be found in Table 1. All electroplating times were fixed at 60 min.

## 2.2. Analysis of the coatings

Prior to surface analysis, all coatings were washed in deionized water and ultrasonicated in acetone for 5 min. Scanning electron microscopy (SEM, JSM-6480LV) was used to observe the surface and the cross-sectional microstructure of the coatings. The particle concentration in the composite coatings was evaluated using an energy dispersive X-ray microanalyzer (EDX) coupled with an SEM. The structures of the coatings were detected via X-ray diffraction using an X'Pert Pro diffractometer (Panalytical). The indentation hardness of the coatings was determined using a Vicker's microhardness indenter with a load of 100 g for 10 s. For the selected load, the substrate effects on hardness could be avoided, and the final value for the hardness of a deposit was given as the average of 5 measurements. The surface scratch hardness of the coatings was measured using a surface property tester (Type 32, SHINTO Scientific, Japan, similar to a JIS K6718 device). The required load of 4.9 N was applied to a conical scratch needle with a tip radius of 5  $\mu\text{m}$ . The needle tip was cleaned with ethanol prior to each scratch test. The final scratch hardness of the coating was evaluated using the scratch width.

Ball-on-disc tests were performed to determine the friction and wear properties of the coatings under dry sliding conditions. The upper specimen, with a diameter of 4.7 mm, was a standard GCr15 steel ball bearing (Shanghai Bearing Corp.) with a hardness of 62–66 HRC and a surface roughness ( $R_a$ ) of 0.025  $\mu\text{m}$ . All tests were performed under a 2-N load with a sliding speed of 0.1 m/s. The friction coefficient and sliding time were recorded automatically during the test. The volumetric loss of the coatings after the friction test was measured using a surface profilometer (Nanomap 500Ls). The specific wear volume of the ball bearings was calculated according to the diameter of the wear scar. The wear rates for all coatings and the material removal rates for the corresponding ball bearings were calculated based on the volumetric loss.

**Table 1**  
Experimental conditions for the composite electrodepositions.

Compositions and conditions	
Nickel sulfate, $\text{NiSO}_4 \cdot 6\text{H}_2\text{O}$ (g/L)	300.0
Nickel chloride, $\text{NiCl}_2 \cdot 6\text{H}_2\text{O}$ (g/L)	45.0
Boric acid, $\text{H}_3\text{BO}_3$ (g/L)	40.0
Particle content (g/L)	0, 5.0
Particle size ( $\mu\text{m}$ )	1–2
sodium dodecyl sulfate (g/L)	0.5
Saccharin sodium (g/L)	1.0
Temperature ( $^\circ\text{C}$ )	45
pH	4 $\pm$ 0.5
Current density ( $\text{A}/\text{dm}^2$ )	2
Magnetic stirring speed (rpm)	200

## 3. Results and discussion

### 3.1. Surface morphology and cross-section observations

The Ni/MoS<sub>2</sub> composite observed after electrophoretic deposition and electrodeposition appears dark in color, and the entire coating is loose with many holes. The branch-like and powdered deposition of the Ni/MoS<sub>2</sub> can be seen in Fig. 1.

Being conductive, these particles are polarized in a current field during the electrophoretic process, and the MoS<sub>2</sub> is deposited onto both the particle surfaces and the cathode, which aids in forming branch-like structures. In addition, a similar process may occur during the second step of the Ni electrodeposition when Ni<sup>2+</sup> ions can easily gain electrons from the outer polarized MoS<sub>2</sub> particles [16]. This mechanism may lead to an undesirable deposit structure and prevents the formation of Ni/MoS<sub>2</sub> composite coatings through a two-step method.

However, quite a different result occurs with Ni/diamond and the two-step method can be used to fabricate these composite coatings. Fig. 2 depicts the surface morphology of a Ni/diamond-2 coating (fabricated via electrophoretic deposition and electrodeposition), with pure Ni and Ni/diamond-1 coatings (fabricated via traditional co-deposition) given for comparison. Fig. 2a indicates that the pure Ni coating has a rather smooth surface with only some spots observed, which may be caused by the addition of brightener. Fig. 2b and c demonstrate the difference in distribution of diamond in the Ni matrix in the composite coatings when using one- and two-step methods. Small pores appear on the surface of co-deposited coating (see Fig. 2b), which could result from the disturbance of hydrogen gas on the matrix surface during the deposition process. Clearly, more diamond particles are embedding in the matrix presented in Fig. 2c than in that shown in Fig. 2b. Although 5 g/L diamond particle concentrations are used in both method, and the plating parameters are identical, the final content of the corresponding coatings is quite different. The EDX analysis indicates a significant increase in diamond particles is obtained using the two-step method over that using the one-step method, and the number particles incorporated in the nickel matrix is approximately two-times higher than that in the Ni/diamond-1.

Representative SEM micrographs of the cross-sectional profiles of the three coatings are depicted in Fig. 3. Distinct variations can be seen in Fig. 3b and c for the diamond particles deposited using the two methods. For the one-step method, the embedded diamond particles exhibit a relatively low concentration in the cross section, and an obvious particle clustering phenomenon appears. However, a relatively homogeneous dispersion of the diamond particles can be observed in the Ni/diamond-2 matrix in Fig. 3c. Though the final electrodeposition times are identical, the thickness of the Ni/diamond-1 and Ni/diamond-2 matrices differ, which may be attributed to their different surface conductivities. Compared with a copper substrate, the presence of a diamond electrophoresis film could negatively impact the electrodeposition process.

The average roughness values were approximately 0.09  $\mu\text{m}$  for a pure Ni coating, 0.46  $\mu\text{m}$  for the Ni/diamond-1 and 0.52  $\mu\text{m}$  for the Ni/diamond-2 coating. The existence of the diamond particles clearly leads to an increase in the roughness, which should be caused by the increased current density at the substrate surface due to the blocking effect of the particles [17].

Fig. 4 presents the XRD patterns for pure Ni, Ni/diamond-1 and Ni/diamond-2 coatings. All the coatings exhibit single phase of Ni matrix with face-centered cubic structure (JCPDS, No. 04-0850). It indicates that the incorporation of diamond particles into the nickel matrix has little effect on the primary structure of the composite coatings.

### 3.2. Indentation hardness and scratch hardness of the coatings

Indentation hardness can be defined as the resistance of a material to local deformation by a vertically penetrating indenter [18]. Fig. 5

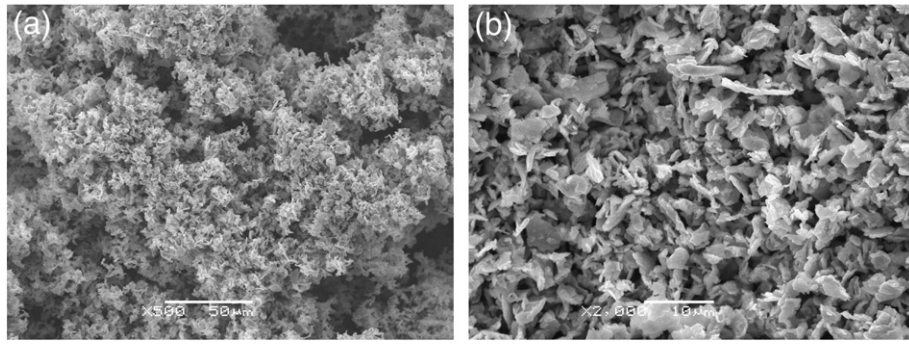


Fig. 1. SEM images of the Ni/MoS<sub>2</sub> coating fabricated via electrophoretic and electrodeposition: (a) low magnification; (b) high magnification.

demonstrates the microhardness of the three coatings. In general, the hardness depends on the incorporation of diamond particles; increasing diamond content in the deposit increases the hardness of the coatings, which can be attributed to the traditional dispersion-strengthening mechanism [9,19]. Another explanation could involve the uniform

distribution of the particles in the nickel matrix, which obstructs the easy movement of the dislocations and resists plastic flow during indentation [20].

The scratch hardness represents the response of the material under a dynamic surface deformation involving a highly localized strain field

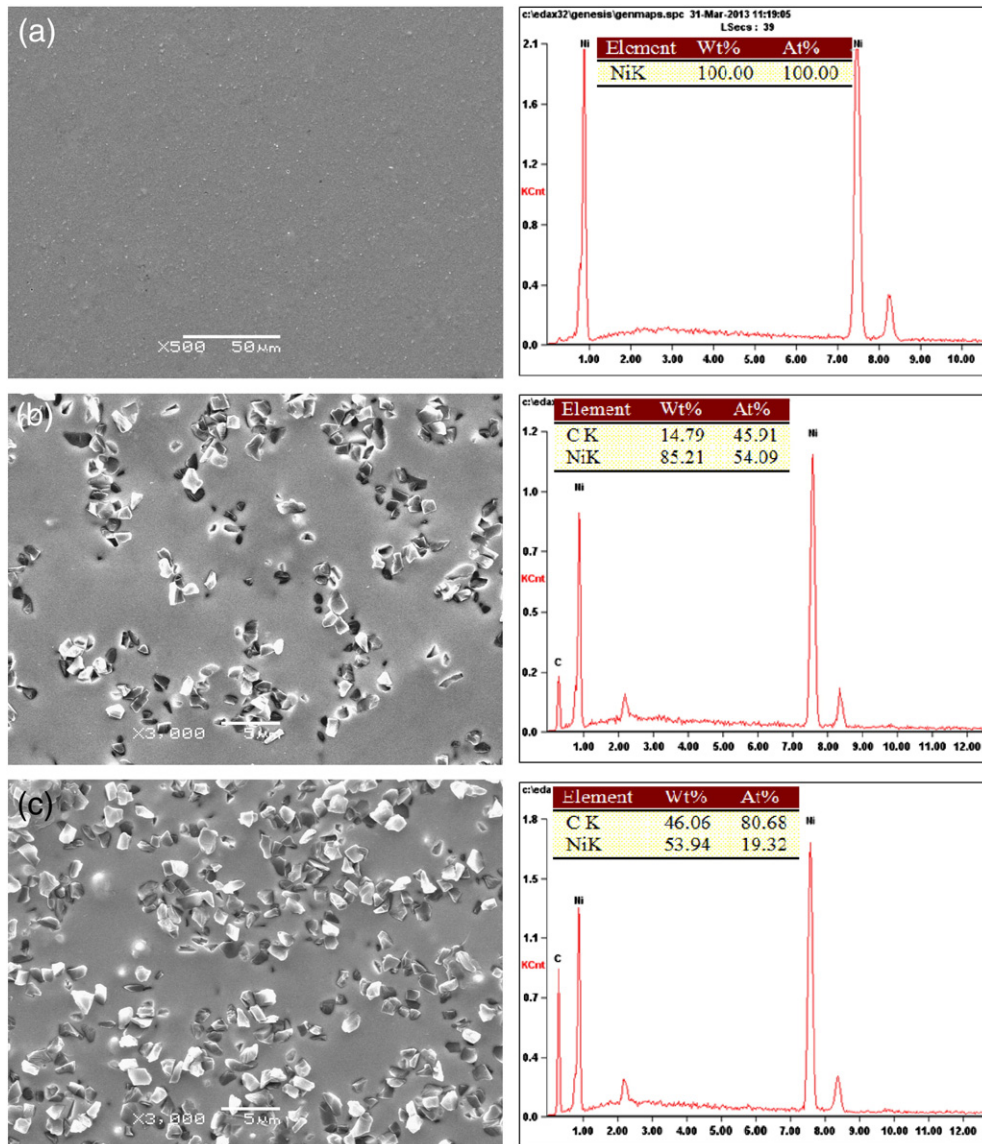


Fig. 2. SEM images and EDX analyses of the three coatings: (a) pure Ni coating; (b) Ni/diamond-1 coating; (c) Ni/diamond-2 coating.

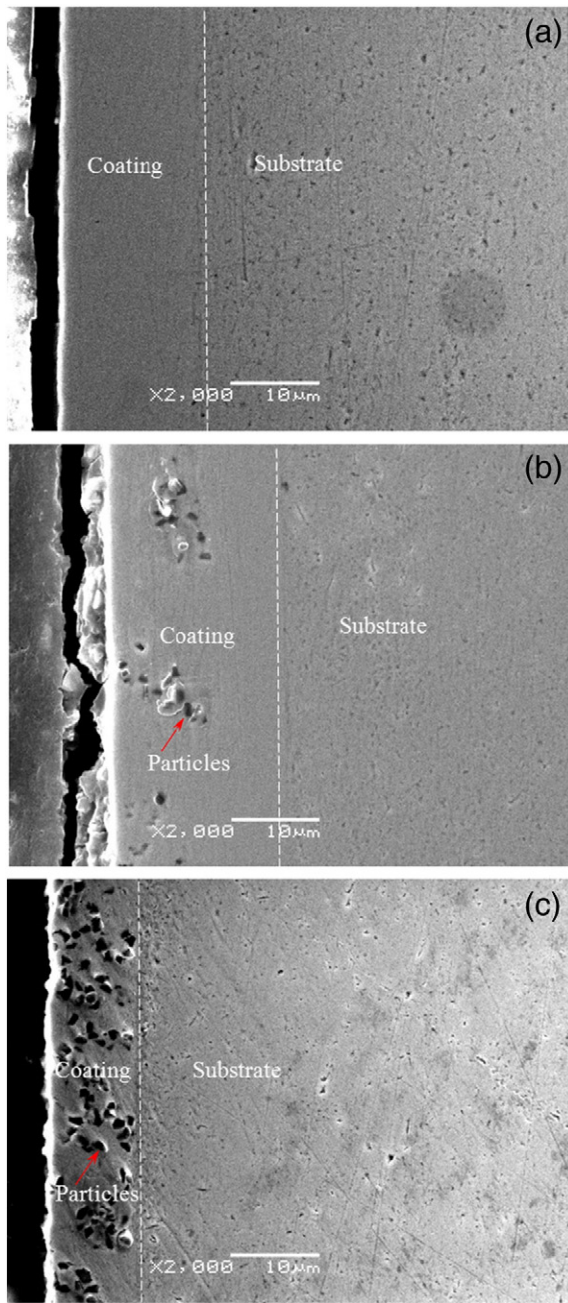


Fig. 3. SEM images presenting the cross sections: (a) pure Ni coating; (b) Ni/diamond-1 coating; (c) Ni/diamond-2 coating.

and material failure [18]. Optical images of the scratch test performed on the three coatings are displayed in Fig. 6. The three trace profiles depict a phenomenon of plastic deformation without failure, indicating that the normal force from the indenter was insufficient to overcome the adhesion between the coating and the substrate. By comparing the scratch width measured on the specimens, a surprising result was obtained: the pure Ni coating exhibited a minimum value of 48  $\mu\text{m}$  despite its possessing the lowest microhardness. The Ni/diamond-2 coating, with the highest microhardness, exhibited the maximum scratch width of 60  $\mu\text{m}$ .

The particles inserted into the matrix act as load-bearing elements; thus, the indentation hardness increases with increasing particle content. However, internal stress greatly affects the scratch properties of the coatings [21]. Given the lattice difference between the particles and matrix, the deposited particles in the coatings can form lattice distortions and defects in the Ni matrix, which significantly enhance the

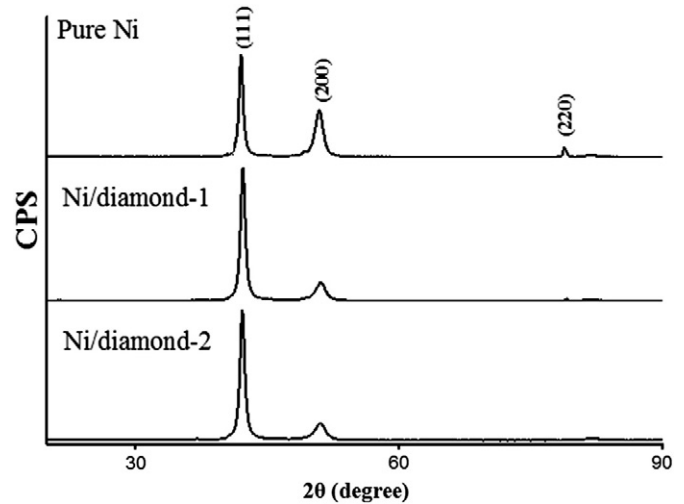


Fig. 4. XRD patterns of the pure Ni and Ni/diamond coatings.

internal stresses on the composite coatings [22], which may account for the low scratch hardness in the Ni/diamond-2 coating.

### 3.3. Tribological performance of the coatings

Fig. 7 shows the friction curve of the Ni-based coatings under dry sliding conditions. The friction coefficients are approximately 0.7–0.9, and the pure Ni exhibits the lowest friction coefficient of the three types of coatings, which is consistent with its lowest hardness. However, although the diamond contents in the coatings are quite different, no differences are observed between the Ni/diamond coatings. In addition, the fluctuating range of the friction curves is significantly higher than that for the pure Ni coatings, which may relate to the surface roughness.

The corresponding wear rates of the pure Ni and Ni/diamond composite coatings are presented in Fig. 8, which indicates that the wear rates of the coatings decrease with increasing diamond content in the metallic matrix and the wear rate of the Ni/diamond-2 coating is approximately half that of the pure Ni coating. As described in the literature [11], the low wear rate of the composite coatings can be attributed to the dispersion-strengthening effect from the incorporation of the diamond particles.

The material removal rate of the GCr15 steel ball bearing increases with increasing diamond content in the corresponding coatings. The removal rate of the ball on the Ni/diamond-2 coating is 8 times higher than that on the Ni coatings (see Fig. 8), which indicates

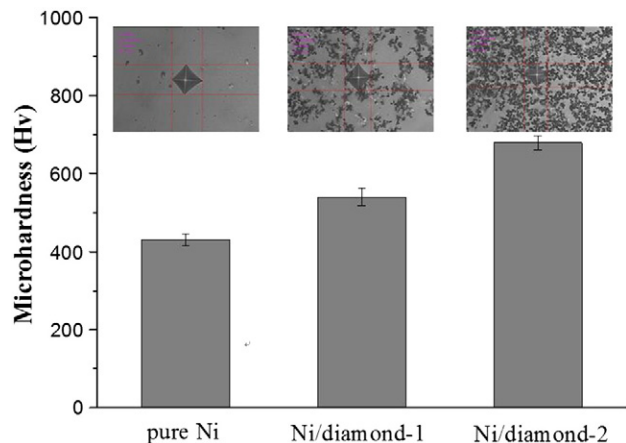


Fig. 5. Microhardness of the three coatings.

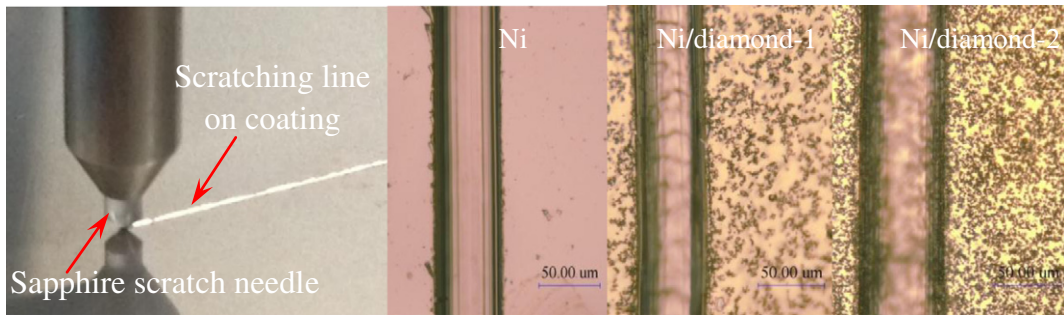


Fig. 6. Scratch hardness and the scratch width images.

that the Ni/diamond coating fabricated using electrophoretic deposition and electrodeposition cannot only inhibit self wear but also increase cutting efficiency.

The improved wear resistance of the co-deposited coatings can also be confirmed using the SEM images of the worn surface depicted in Fig. 9. For the pure Ni coating, distinct scratches, delaminations and some plastic deformations are found along the wear track, and heavy peeling occurs in the bulk (see Fig. 9a), indicating a possible adhesive wear mechanism. Scaling is the predominant form of wear on the co-deposited coatings. As illustrated in Fig. 9b and c, the adhesion wear

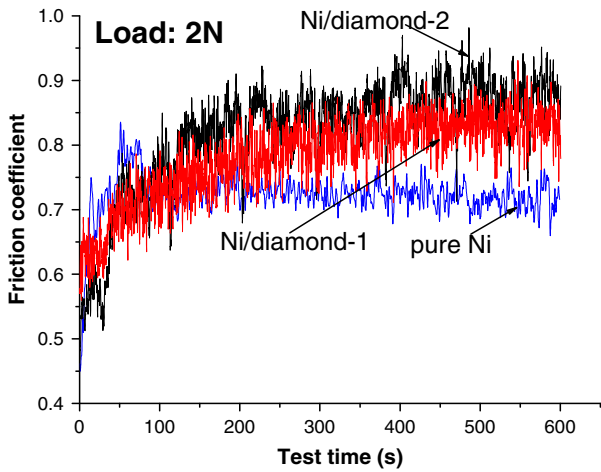


Fig. 7. The friction curves of the Ni-based coatings under dry sliding conditions.

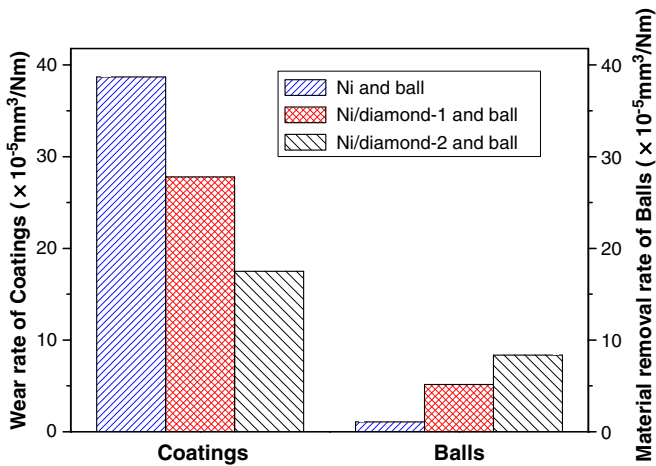


Fig. 8. Wear rates of coatings and corresponding material removal rate of the balls.

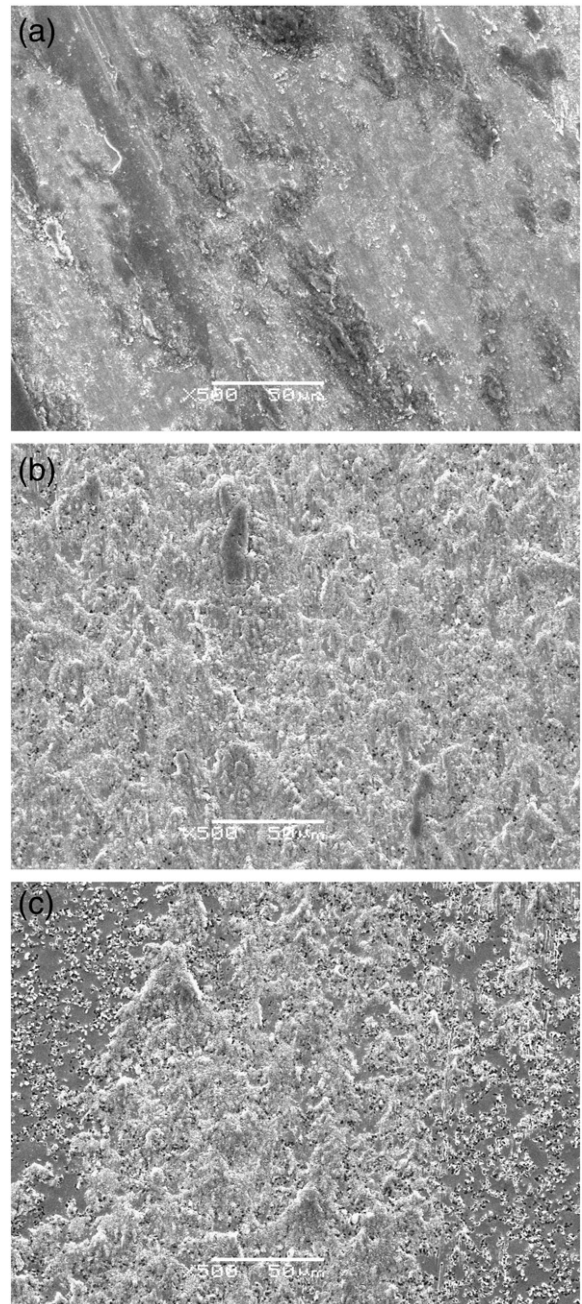


Fig. 9. SEM images of the worn coating surfaces under dry sliding conditions: (a) pure Ni coating; (b) Ni/diamond-1 coating; (c) Ni/diamond-2 coating.

and scuffing on the worn surfaces of the composite coatings decrease to some degree, especially for the Ni/diamond-2 coating (see Fig. 9c). As indicated in Fig. 9b and c, the wrinkled and damaged areas on the worn composite coatings are reduced over those in Fig. 9a, and the embedded diamond particles can be observed under the wear scar.

The wear resistance of the Ni/diamond-2 is superior to that of the Ni/diamond-1 coating, due to not only the content but also the manner in which the particles are incorporated within the matrix. For the Ni/diamond-2 coatings, the deposited nickel occupies the space formed in the diamond film via electrophoresis; thus, the diamond particles are tightly held and strongly bonded within the matrix. While for the Ni/diamond-1, the specific surface interactions during the co-deposition should be regarded as a dynamic process with the co-deposition of the particles taking place on a renewable surface. Interfacial bonding strength between the diamond and the matrix is relatively low and may affect its wear property. The Ni/diamond-2 coating was found to possess excellent cutting performance from the perspective of material removal. Because diamond is far harder than a steel ball, the particles on the coating surface act as many micro-cutters to improve material remove. The increased particle concentration on the surface of the Ni/diamond-2 coating could provide another explanation for the increased material removal rate.

#### 4. Conclusion

Electrophoretic deposition combined with electrodeposition is a suitable technique for producing composite coatings with high particle concentrations. To verify its feasibility, typical non-conductive diamond and conductive molybdenum disulfide were chosen to fabricate composite coatings via electrophoretic deposition and electrodeposition. The effects of the fabrication techniques on the coating morphologies, hardness and tribological performance were investigated and the following conclusions obtained:

- (1) With the conductive MoS<sub>2</sub> particles, no Ni/MoS<sub>2</sub> composite coatings can be achieved via the two-step method under the given conditions. However, the Ni/diamond coating can be prepared when using the electrophoretic deposition and electrodeposition technique. Compared with conventional co-deposition methods, the diamond content was effectively enhanced.

- (2) The Vicker's indentation hardness increased with increasing diamond content in the Ni/diamond coatings, whereas the opposite trend was observed in the scratch hardness.
- (3) Compared with pure Ni and Ni/diamond-1, the wear resistance of the Ni/diamond coating prepared via the electrophoretic deposition and electrodeposition technique was effectively improved, and the material removal rate of the opposite ball bearing increased significantly.

#### Acknowledgments

This research is supported by NUAA Research Funding (NP2013306).

#### References

- [1] M. Stroumbouli, P. Gyftou, E.A. Pavlatou, N. Spyrellis, *Surf. Coat. Technol.* 195 (2005) 325–332.
- [2] E. Pompei, L. Magagnin, N. Lecis, P.L. Cavallotti, *Electrochim. Acta* 54 (2009) 2571–2574.
- [3] B.R. Tian, Y.F. Cheng, *Electrochim. Acta* 53 (2007) 511–517.
- [4] B. Szczygieł, M. Kołodziej, *Electrochim. Acta* 50 (2005) 4188–4195.
- [5] M. Lekka, A. Lanzutti, C. Zanella, G. Zendron, L. Fedrizzi, P.L. Bonora, *Pure Appl. Chem.* 83 (2011) 295–308.
- [6] Q. Feng, T. Li, H. Teng, X. Zhang, Y. Zhang, C. Liu, J. Jin, *Surf. Coat. Technol.* 202 (2008) 4137–4144.
- [7] L. Shi, C. Sun, W. Liu, *Appl. Surf. Sci.* 254 (2008) 6880–6885.
- [8] T.W. Tomaszewski, *Trans. Inst. Met. Finish.* 54 (1976) 45–48.
- [9] A. Hovestad, L.J.J. Janssen, *J. Appl. Electrochem.* 25 (1995) 519–527.
- [10] A.K. Sikder, T. Sharda, D.S. Misra, D. Chandrasekaram, P. Veluchamy, H. Minoura, P. Selvam, *J. Mater. Res.* 14 (1999) 1148–1152.
- [11] L.P. Wang, Y. Gao, H.W. Lui, Q.J. Xue, T. Xu, *Surf. Coat. Technol.* 191 (2005) 1–6.
- [12] N.K. Shrestha, T. Takebe, T. Saji, *Diam. Relat. Mater.* 15 (2006) 1570–1575.
- [13] N.K. Shrestha, K. Sakurada, M. Masuko, T. Saji, *Surf. Coat. Technol.* 140 (2001) 175–181.
- [14] S. Teruyama, N.K. Shrestha, Y. Ito, M. Iwanaga, T. Saji, *J. Mater. Sci.* 39 (2004) 2941–2943.
- [15] H. Ogihara, A. Hara, K. Miyamoto, N.K. Shrestha, T. Kaneda, S. Itob, T. Saji, *Chem. Commun.* 46 (2010) 442–444.
- [16] Z.J. Huang, D.S. Xiong, *Surf. Coat. Technol.* 202 (2008) 3208–3214.
- [17] R. Balaji, M. Pushpavanam, K.Y. Kumar, K. Subramanian, *Surf. Coat. Technol.* 201 (2006) 3205–3211.
- [18] S.K. Sinha, T. Song, X. Wan, Y. Tong, *Wear* 266 (2009) 814–821.
- [19] I. Garcia, J. Fransaer, J.P. Celis, *Surf. Coat. Technol.* 148 (2001) 171–178.
- [20] M. Pushpavanam, S.R. Natarajan, *Metal Finishing*, 1995, 97–99.
- [21] M.H. Blees, G.B. Winkelman, A.R. Balkenende, J.M.J.d. Toonder, *Thin Solid Films* 359 (2000) 1–13.
- [22] S. Shi, L.M. Chang, *J. Jilin Univ.* 4 (2006) 46–48, (NaturalScience Edition).